PHYSICAL REVIEW B **97**, 060304(R) (2018)

Rapid Communications

Dynamical topological invariant after a quantum quench

Chao Yang,[1,2] Linhu Li,[3] and Shu Chen[1,2,4,*]

[1]*Beijing National Laboratory for Condensed Matter Physics, Institute of Physics, Chinese Academy of Sciences, Beijing 100190, China*
[2]*School of Physical Sciences, University of Chinese Academy of Sciences, Beijing 100049, China*
[3]*Department of Physics, National University of Singapore, Singapore 117542, Singapore*
[4]*Collaborative Innovation Center of Quantum Matter, Beijing, China*

(Received 11 October 2017; published 26 February 2018)

We show how to define a dynamical topological invariant for one-dimensional two-band topological systems after a quantum quench. By analyzing general two-band models of topological insulators, we demonstrate that the reduced momentum-time manifold can be viewed as a series of submanifolds S^2, and thus we are able to define a dynamical topological invariant on each of the spheres. We also unveil the intrinsic relation between the dynamical topological invariant and the difference in the topological invariant of the initial and final static Hamiltonian. By considering some concrete examples, we illustrate the calculation of the dynamical topological invariant and its geometrical meaning explicitly.

DOI: 10.1103/PhysRevB.97.060304

Introduction. In the last decade, the study of topological quantum matter is one of the most attractive topics in condensed matter physics [1–5], and our knowledge of topological properties for various quantum systems has been widely expanded. In contrast to equilibrium systems, what we know about topological quantum matter out of equilibrium is quite rare [6]. Topology properties far from equilibrium have been studied in different ways, such as the dynamics of edge states [7–9], dynamical quantum phase transitions [10–12], Floquet topological states [13–15], etc. The rapid development of cold atom experiments provides a powerful tool to study the dynamics far from equilibrium [16–19], and the evolution of a quantum state can be visualized with the method of Bloch state tomography [20–22].

A typical example of dynamics far from equilibrium is the quantum quench. Initially, the state is prepared in the ground state of Hamiltonian H^i, and then a quench to the system is carried out by suddenly changing a physical parameter, denoted by a new Hamiltonian H^f. It is known that the topological invariant will remain unchanged because the time evolution operator is unitary [23–25], and the topology of the final Hamiltonian does not influence the topology of the time-evolved state. However, the nonequilibrium topological response is found to exhibit some novel properties with no equilibrium analog [26–29]. Also, it has recently been shown that the topology of the final Hamiltonian can be reflected by the Hopf invariant in a two-dimensional (2D) Chern insulator [25,30,31], which gives a first example in defining the topological invariant far from equilibrium. It is still a challenge to understand how to explore the nontrivial topology properties of a dynamic system in a general way.

In this Rapid Communication, we study general two-band nonequilibrium systems in one dimension (1D), and extract a dynamical topological invariant defined on the momentum-time manifold. A 2D torus T^2 composed of momentum and time can be reduced into a series of spheres (S^2), and a dynamical Chern number is achieved from each of the spheres. This Chern number measures how many times the Bloch sphere is covered when the time-evolved Bloch vector winds over the corresponding sphere. We also analyze the intrinsic relation between the dynamical topological invariant and the topology of H^i and H^f in equilibrium and give some examples to explain our results. At last, we point out that a dynamical topological invariant can be visualized experimentally.

Model and quench dynamics. We consider a general 1D two-band tight-binding model, and at each momentum k the Hamiltonian is described by

$$h(k) = d_0(k)\mathbf{I} + \mathbf{d}(k)\cdot\boldsymbol{\sigma}, \tag{1}$$

where $\mathbf{I}$ is the 2×2 identity matrix and $\boldsymbol{\sigma} = (\sigma_x,\sigma_y,\sigma_z)$ are Pauli matrices acting on a (pseudo) spin-1/2 space. This model can be used to describe a variety of topological insulators and superconductors, for example, the Su-Schrieffer-Hegger (SSH) model [32] and the p-wave Kitaev chain [33]. The eigenvalues are given by

$$\epsilon_\pm(k) = d_0(k) \pm |\mathbf{d}(k)|, \tag{2}$$

and we denote the eigenvectors as $|\psi_\pm(k)\rangle$. For convenience, we use the corresponding density matrices instead of the state vectors, which read

$$\hat{\rho}_\pm(k) = |\psi_\pm(k)\rangle\langle\psi_\pm(k)| = \tfrac{1}{2}[1 \pm \hat{\mathbf{d}}(k)\cdot\boldsymbol{\sigma}], \tag{3}$$

where $\hat{\mathbf{d}}(k) = \frac{\mathbf{d}(k)}{|\mathbf{d}(k)|}$ is the normalized vector localized on the Bloch sphere S^2. The topological invariant of the system can be calculated with the information of $\hat{\mathbf{d}}(k)$ for both $\mathbb{Z}$ and $\mathbb{Z}_2$ types in one dimension [5].

Now, we study the dynamical properties of the system far from equilibrium. By preparing the system in the ground state of the initial Hamiltonian h^i, i.e., $\rho^i(k) = \frac{1}{2}[1 - \hat{\mathbf{d}}^i(k)\cdot\boldsymbol{\sigma}]$, and

*Corresponding author: schen@iphy.ac.cn

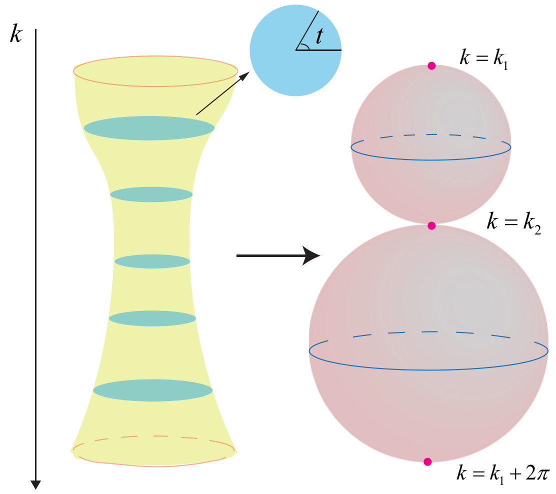

FIG. 1. Scheme of the momentum-time manifold. In the left figure, for any fixed momentum k, the cross section can be viewed as a circle S^1 where the azimuthal angle represents the time t. After gluing $k = 0$ and $k = 2\pi$ (saffron circles), the topology of the momentum-time manifold becomes T^2. If there are two fixed points $k = k_1$ and k_2, the corresponding circle contracts to a point, then the momentum-time manifold can be reduced to a series of spheres S^2.

then performing a sudden quench to the final Hamiltonian h^f, the evolution of density matrices can be written as

$$\rho(k,t) = \tfrac{1}{2}[1 - \hat{\boldsymbol{d}}(k,t)\cdot\boldsymbol{\sigma}], \tag{4}$$

with $\hat{\mathbf{d}}(k,t)$ achieved from the Liouville–von Neumann equation,

$$\hat{\mathbf{d}}(k,t) = \hat{\mathbf{d}}^i \cos(2|\mathbf{d}^f|t) + 2\hat{\mathbf{d}}^f\left(\hat{\mathbf{d}}^i\cdot\hat{\mathbf{d}}^f\right)\sin^2(|\mathbf{d}^f|t) + \hat{\mathbf{d}}^i\times\hat{\mathbf{d}}^f\sin(2|\mathbf{d}^f|t), \tag{5}$$

where $\hat{\mathbf{d}}^i$ and $\hat{\mathbf{d}}^f$ are Bloch vectors of the initial and final Hamiltonians [34], both of them being functions of momentum k. Equation (5) can be interpreted as the winding of $\hat{\mathbf{d}}$ from the initial vector $\hat{\mathbf{d}}^i$ around the axis $\hat{\mathbf{d}}^f$ on the Bloch sphere during the evolution process. The Berry phase of the time-dependent wave function does not change after taking a global quench due to the evolution being unitary [23], hence it cannot characterize the topological difference between H^i and H^f. In the following, we shall explore how to define a unique topological quantity to characterize topologically different quench dynamics.

General definition of dynamical topological invariant. To unveil the dynamical properties after a sudden quench, we first study a manifold composed of momentum and time. In general, the 1D Brillouin zone (BZ) has a topology S^1. Furthermore, it can be seen from Eq. (5) that the time evolution of density matrices has a periodicity $\frac{\pi}{|\mathbf{d}^f|}$ for each momentum k. After rescaling the time $t' = \frac{t}{|\mathbf{d}^f|}$, the topology of time can be viewed as S^1, hence the total momentum-time manifold has a topology T^2, as shown in the left column of Fig. 1.

However, the momentum-time manifold is more complicated for topologically nontrivial 1D systems. Suppose that there exist some momenta, at which $\mathbf{d}^i(k)$ are parallel or antiparallel to $\mathbf{d}^f(k)$, then the Bloch vectors $\hat{\mathbf{d}}(k,t)$ will remain at the initial points $\mathbf{d}^i(k)$ according to Eq. (5), and the corresponding eigenvectors $|\psi_-(k)\rangle$ will not evolve with time apart from a global phase. For topologically nontrivial systems, there must exist some "fixed points," which are ensured by symmetries protecting the 1D topological state, as will be further clarified later in specific cases belonging to different symmetry classes. In the right column in Fig. 1, we assume $k = k_1$ and k_2 are fixed points, at which the time axis can be contracted to a point as the Bloch vectors keep still during the time evolution. Therefore, the topology of the momentum-time manifold is reduced to two spheres [35]. In general, if there are N fixed points in a BZ, the momentum-time manifold T^2 can be reduced to N submanifolds, each of them having a topology S^2.

Now, we naturally have a map from each momentum-time submanifold to the Bloch vector $\hat{\mathbf{d}}(k,t)$, which is $S^2 \to S^2$, and then we can define a Chern number,

$$C^m_{\mathrm{dyn}} = \frac{1}{4\pi}\int_{k_m}^{k_{m+1}} dk \int_0^{\pi} dt' (\hat{\mathbf{d}}\times\partial_{t'}\hat{\mathbf{d}})\cdot\partial_k,\hat{\mathbf{d}}, \tag{6}$$

where $m = 1,2,\ldots,N$ denotes the mth submanifold, k_m denotes the mth fixed point, and $k_{N+1} = k_1 + 2\pi$ is the same point modulo 2π. Hence the integral is an integer and it measures how many times the Bloch vectors cover the unit sphere.

By a straightforward calculation [34], the dynamical topological invariant can be written as

$$C^m_{\mathrm{dyn}} = \tfrac{1}{2}\left(\cos\theta_{k=k_m} - \cos\theta_{k=k_{m+1}}\right), \tag{7}$$

where θ_k is the included angle between $\hat{\mathbf{d}}^i(k)$ and $\hat{\mathbf{d}}^f(k)$. This invariant only contains the information about the fixed points $k = k_m$ and $k = k_{m+1}$, and depends only on the included angle of the initial and final Hamiltonian. Exchanging the initial and final parameters $\mathbf{d}^{i(f)} \to \mathbf{d}^{f(i)}$ will not affect the dynamical topological invariant. On the other hand, the included angle θ_{k_m} can only take a value 0 or π as $\mathbf{d}^i(k)$ is parallel or antiparallel to $\mathbf{d}^f(k)$, hence the dynamical topological invariant can only be $C^m_{\mathrm{dyn}} = 0$ for $\theta_{k_m} = \theta_{k_{m+1}}$, or $C^m_{\mathrm{dyn}} = \pm 1$ for $\theta_{k_m} = \theta_{k_{m+1}} + \pi(\mathrm{mod}\, 2\pi)$.

For any $m \in 1,2,\ldots,N$, the mapping from the corresponding momentum-time submanifold to the Bloch vectors induces a dynamical topological invariant C^m_{dyn}, and $C^m_{\mathrm{dyn}} = 0$ (± 1) indicates that the mapping is trivial (nontrivial). The number of nontrivial mappings is related to the topological properties of the initial and final systems. In the following, we will unveil these relations by studying specific topological classes of the tenfold way symmetry classification [36,37]. According to this classification, for 1D two-band systems with no internal spin degree, only three types, i.e., classes of BDI, AIII, and D, are topologically nontrivial.

Class BDI and AIII. In 1D, systems of class BDI and AIII preserve chiral symmetry, hence the topological invariants are characterized by the winding number, and the relation between the number of nontrivial mappings M and the winding numbers in equilibrium is given by the following theorem.

Theorem 1. In class BDI and AIII, the number of nontrivial mappings M from momentum-time submanifolds to Bloch vectors has a lower bound $2|n^i - n^f|$, with n^i and n^f being the winding numbers of H^i and H^f, respectively.

See the Supplemental Material [34] for the proof and details. Note that M can reflect the difference in winding numbers between the initial and final Hamiltonians. If $n^i \neq n^f$, the nontrivial mappings cannot be removed simultaneously under continuous deformation because the winding number in equilibrium is protected by symmetry. In most of the examples which we have seen there are only two fixed points, so it can be found from Eq. (7) that the dynamical topological invariants satisfy $C^1_{\rm dyn} = -C^2_{\rm dyn}$, and then we only need to know the $m = 1$ submanifold; we therefore have the following corollary from Theorem 1.

Corollary 1. Consider a Hamiltonian in class BDI and AIII, suppose that there are only two fixed points, and then the dynamical topological invariant $C^1_{\rm dyn} = \pm 1$ if H^i and H^f lie in different topological phases.

From Corollary 1 we find that the dynamical topological invariant $C^1_{\rm dyn}$ is closely related to the topological properties of both H^i and H^f. To see it clearly, next we study a concrete example by considering the famous SSH model [32,38], which belongs to the class BDI and is described by the Hamiltonian

$$H = \sum_i [(t+\delta)\hat{c}^\dagger_{A,i}\hat{c}_{B,i} + (t-\delta)\hat{c}^\dagger_{A,i+1}\hat{c}_{B,i}] + \text{H.c.}, \quad (8)$$

where $\hat{c}^\dagger_{A(B),i}$ is the creation operator of the fermion on the ith A (or B) sublattice. After the Fourier transformation $\hat{c}_{s,j} = \frac{1}{\sqrt{L}}\sum_k e^{ikj}\hat{c}_{k,s}$ with $s = A(B)$ and setting $t = 1$, the Hamiltonian can be written as

$$H = \sum_k \psi^\dagger_k h(k) \psi_k, \quad (9)$$

where $\psi^\dagger_k = (\hat{c}^\dagger_{k,A}, \hat{c}^\dagger_{k,B})$ and $h(k) = d_x\sigma_x + d_y\sigma_y$, with $d_x = (1+\delta) + (1-\delta)\cos k$ and $d_y = (1-\delta)\sin k$. For $\delta > 0$, the half-filled system is topologically trivial, whereas for $\delta < 0$ the system is topological. It can be seen for any δ^i and δ^f that there are only two fixed points $k_1 = 0$ and $k_2 = \pi$, corresponding to two high-symmetry points [39], and the total Brillouin zone is reduced to two spheres denoted by $m = 1,2$ with $k \in (0,\pi)$ and $k \in (\pi, 2\pi)$, respectively.

Suppose that both δ^i and δ^f lie in the same phase, either topologically nontrivial or trivial, and the Bloch vectors satisfy $\hat{\mathbf{d}}^i(0) = \hat{\mathbf{d}}^f(0)$ and $\hat{\mathbf{d}}^i(\pi) = \hat{\mathbf{d}}^f(\pi)$. According to Eq. (7), we have $C^1_{\rm dyn} = C^2_{\rm dyn} = 0$, hence the number of nontrivial mappings is zero, which equals the difference in the winding numbers between the initial and final Hamiltonians. On the other hand, if δ^i and δ^f are in different phases, we find $\hat{\mathbf{d}}^i(0) = \hat{\mathbf{d}}^f(0)$ and $\hat{\mathbf{d}}^i(\pi) = -\hat{\mathbf{d}}^f(\pi)$. The dynamical topological invariants are $C^1_{\rm dyn} = -1$ and $C^2_{\rm dyn} = 1$, indicating that both of the mappings are topologically nontrivial. Our results show that the number of nontrivial mappings in the SSH model is $M = 2|n^i - n^f|$, in accordance with Theorem 1.

Because there are only two fix points in the Hamiltonian, it is sufficient to study the submanifold $m = 1$ from Corollary 1. In order to get an intuitive understanding of the geometrical meaning of the dynamical Chern number, in Fig. 2 we show the evolution of Bloch vectors for different choices of the initial and final parameters for the submanifold $m = 1$. Each solid loop represents the trajectory of a definite mode in a period. After collecting all trajectories for $k \in (0,\pi)$ into the Bloch sphere, the topological properties can be directly obtained. In

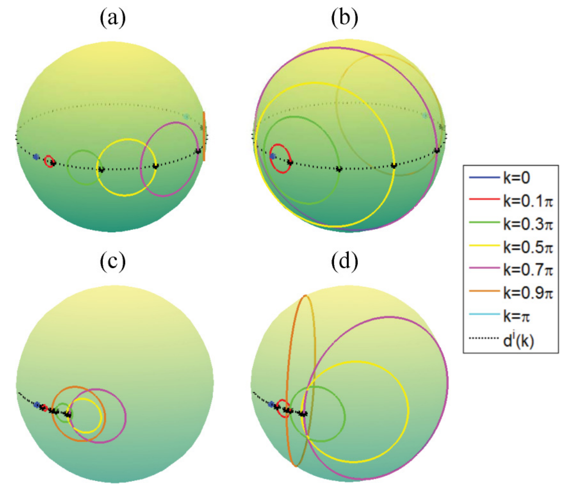

FIG. 2. The evolution of the Bloch vector for different momenta in a period, with (a) $\delta^i = -0.7$ and $\delta^f = -0.3$; (b) $\delta^i = -0.7$ and $\delta^f = 0.3$; (c) $\delta^i = 0.4$ and $\delta^f = 0.2$; and (d) $\delta^i = 0.4$ and $\delta^f = -0.2$. The black dotted loop represents the distribution of initial Bloch vectors $\hat{\mathbf{d}}^i(k)$, corresponding to topological cases in (a) and (b) and trivial cases in (c) and (d). The black stars at the crossing points represent the initial points at $t = 0$ of each loop.

Figs. 2(a) and 2(c), both δ^i and δ^f lie in the same phase, and the trajectories of different Bloch vectors cancel each other out, giving rise to the dynamical Chern number $C^1_{\rm dyn} = 0$; however, in Figs. 2(b) and 2(d), δ^i and δ^f lie in different phases, and the trajectories for the Bloch vectors of $k \in (0,\pi)$ cover the whole Bloch sphere, corresponding to $C^1_{\rm dyn} = -1$.

Class D. In class D, the particle-hole symmetry constrains the direction of the Bloch vector $\hat{\mathbf{d}}(k)$ lying on the z axis at $k = 0$ and $k = \pi$ [33], hence they are fixed points and the momentum-time submanifolds are reduced to two spheres denoted by $m = 1,2$. The Z_2 topological invariant for static 1D systems in class D can be defined as $n = \text{sgn}[d_z(0)d_z(\pi)]$, where $n = -1$ for the topological phase and $n = 1$ for the trivial phase. Similar to class BDI and AIII, we can prove [34] the following theorem.

Theorem 2. Consider a Hamiltonian in class D. The dynamical topological invariant $C^1_{\rm dyn} = 0$ if H^i and H^f lie in the same phase; in contrast, $C^1_{\rm dyn} = \pm 1$ if H^i and H^f lie in different phases.

For a system of class D, since there exist solely two fixed points $k = 0$ and π, protected by particle-hole symmetry, thus we only need to calculate the dynamical topological invariant of submanifold $m = 1$. A simple example of a D class system is the extended version of the 1D Kitaev model described by Hamiltonian (1) with $d_0 = 0$, $d_x = \Delta_2 \sin\phi \sin 2k$, $d_y = \Delta_1 \sin k + \Delta_2 \cos\phi \sin 2k$, and $d_z = -t_1 \cos k - t_2 \cos 2k + \mu$ [33,40], where t_1 and t_2 represent the nearest-neighbor (NN) and next-nearest-neighbor (NNN) hopping amplitudes, Δ_1 and Δ_2 the NN and NNN pairing parameters, ϕ denotes the phase difference of the two pairing parameters, and μ the chemical potential. For simplicity, we take $\mu = 1$, $\Delta_1 = t_1 = 0.5$, $\phi = \frac{\pi}{2}$, and $\Delta_2 = t_2 \equiv \Delta$. It was shown that the system is topological when $0.5 < \Delta < 1.5$, with Majorana fermions emerging at

TABLE I. Dynamical topological invariant for different initial and final phases. For convenience, we label the interval $\Delta < 0.5$ by I, $0.5 < \Delta < 1.5$ by II, and $\Delta > 1.5$ by III, hence the interval II is the topological phase, the intervals I and III are topological trivial phases, and $m = 1,2$ label the momentum-time submanifolds.

Initial to final phases	$m = 1$	$m = 2$
I → I	0	0
I → II	1	−1
I → III	0	0
II → II	0	0
II → III	−1	1
III → III	0	0

the boundaries, whereas the system is trivial for $\Delta < 0.5$ and $\Delta > 1.5$. The fixed points $k = 0$ and π are protected by particle-hole symmetry, and explicitly we have $\hat{\mathbf{d}}(k=0) = [0,0,\mathrm{sgn}(0.5-\Delta)]$ and $\hat{\mathbf{d}}(k=\pi) = [0,0,\mathrm{sgn}(1.5-\Delta)]$. By using formula (7), we can directly calculate the dynamical topological invariant. Because both the intervals $\Delta < 0.5$ and $\Delta > 1.5$ are topologically trivial, there are more choices for initial and final parameters. The dynamical topological invariants are shown in Table I, indicating that the nontrivial dynamical topological invariant appears only when Δ^i and Δ^f lie in topologically different phases.

To get a geometrical understanding, in Fig. 3 we show the evolution of Bloch vectors for different choices of Δ^i and Δ^f. In class D, though the initial states (black dotted curve) do not lie on an orthodrome, and the trajectories seem to be more complicated, we can always find the Bloch sphere being fully covered in Figs. 3(b) and 3(d) with Δ^i and Δ^f located in different phases, while all the trajectories cancel each other out in Figs. 3(a) and 3(c) with Δ^i and Δ^f located in the same phase.

A topologically trivial example. As a comparison, we study a 1D tight-binding model with alternating chemical potentials μ and $-\mu$ on the A and B sublattice, which is described by Hamiltonian (9) with $d_x = 1 + \cos k$, $d_y = \sin k$, and $d_z = \mu$. The system carries out a quantum phase transition at $\mu = 0$, which is just the gap-closing point. This model describes a topologically trivial system as it always has no nontrivial Berry phase [41]. We find that there exists only an accidental fixed point $k = \pi$, and thus the dynamical topological invariant should be calculated in the whole BZ. According to formula (7), the dynamical topological invariant $C^1_{\mathrm{dyn}} = 0$ for arbitrary μ^i and μ^f, suggesting that no nontrivial mappings from the momentum-time manifold to Bloch vectors exist in this model.

Finally, we point out that the dynamical topological invariant is in principe measurable in current cold atom experiments.

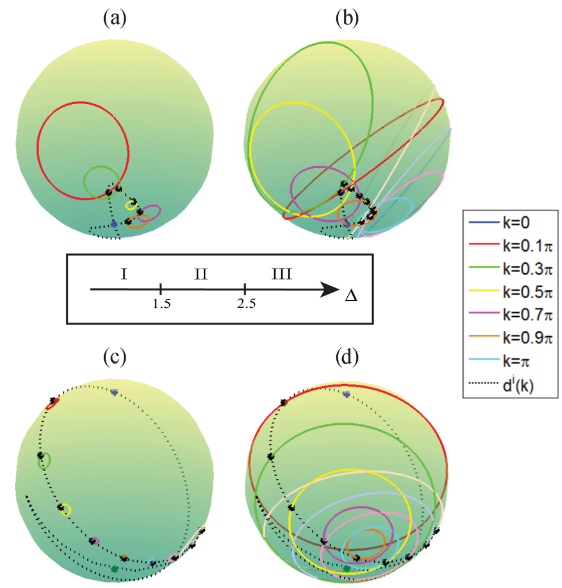

FIG. 3. The evolution of the Bloch vector for different momenta in a period, with (a) $\Delta^i = 0.2$ and $\Delta^f = 0.4$; (b) $\Delta^i = 0.2$ and $\Delta^f = 1.4$; (c) $\Delta^i = 1.4$ and $\Delta^f = 1.2$; and (d) $\Delta^i = 1.4$ and $\Delta^f = 0.2$. The black dotted loop denotes the distribution of initial Bloch vectors $\hat{\mathbf{d}}^i(k)$, corresponding to the trivial case in (a) and (b) and the topological case in (c) and (d). The black stars at the crossing points represent the initial points at $t = 0$ of each loop. The middle inset gives the phase diagram of the static system.

If the energy band of H^f is a flatband, i.e., SSH model with $\delta^f = \pm 1$, all the momenta have the same period. With the technique of Bloch state tomography [20–22], the evolution of the state in BZ can be observed in a period. After collecting the trajectories in a definite momentum-time submanifold m, the dynamical topological invariant can be measured directly.

Summary. In summary, we have clarified how to properly define a dynamical topological invariant for a general 1D two-band insulator system performed by a quantum quench. After showing that the momentum-time manifold can be reduced to a series of spheres, a dynamical topological invariant can be defined for the mapping from each of the spheres to the Bloch vectors. Then we analyzed the intrinsic relation between the dynamical topological invariant and the topological invariant of H^i and H^f in equilibrium. We also gave some visualized examples to show our results. Finally, we pointed out that the dynamical topological invariant is experimentally measurable.

Acknowledgments. The work is supported by NSFC under Grant No. 11425419, the National Key Research and Development Program of China (2016YFA0300600) and 2016YFA0302104)), and the Strategic Priority Research Program (B) of the Chinese Academy of Sciences (Grant No. XDB07020000).

[1] M. Z. Hasan and C. L. Kane, Rev. Mod. Phys. **82**, 3045 (2010).
[2] X. Qi and S. Zhang, Rev. Mod. Phys. **83**, 1057 (2011).
[3] A. Bansil, H. Lin, and T. Das, Rev. Mod. Phys. **88**, 021004 (2016).
[4] E. Witten, Rev. Mod. Phys. **88**, 035001 (2016).
[5] C. Chiu, J. C. Y. Teo, A. P. Schnyder, and S. Ryu, Rev. Mod. Phys. **88**, 035005 (2016).
[6] J. Eisert, M. Friesdorf, and C. Gogolin, Nat. Phys. **11**, 124 (2015).

[7] A. Bermudez, D. Patane, L. Amico, and M. A. Martin-Delgado, Phys. Rev. Lett. **102**, 135702 (2009).
[8] A. Rajak and A. Dutta, Phys. Rev. E **89**, 042125 (2014); P. D. Sacramento, *ibid.* **90**, 032138 (2014).
[9] P. D. Sacramento, Phys. Rev. E **93**, 062117 (2016).
[10] S. Vajna and B. Dóra, Phys. Rev. B **91**, 155127 (2015).
[11] J. C. Budich and M. Heyl, Phys. Rev. B **93**, 085416 (2016).
[12] Z. Huang and A. V. Balatsky, Phys. Rev. Lett. **117**, 086802 (2016).
[13] N. H. Lindner, G. Rafael, and V. Galitski, Nat. Phys. **7**, 490 (2011).
[14] L. Jiang, T. Kitagawa, J. Alicea, A. R. Akhmerov, D. Pekker, G. Refael, J. I. Cirac, E. Demler, M. D. Lukin, and P. Zoller, Phys. Rev. Lett. **106**, 220402 (2011).
[15] A. Gómez-León and G. Platero, Phys. Rev. Lett. **110**, 200403 (2013).
[16] M. Aidelsburger, M. Atala, M. Lohse, J. T. Barreiro, B. Paredes, and I. Bloch, Phys. Rev. Lett. **111**, 185301 (2013).
[17] G. Jotzu, M. Messer, R. Desbuquois, M. Lebrat, T. Uehlinger, D. Greif, and T. Esslinger, Nature (London) **515**, 237 (2014).
[18] M. Atala, M. Aidelsburger, J. T. Barreiro, D. Abanin, T. Kitagawa, E. Demler, and I. Bloch, Nat. Phys. **9**, 795 (2013).
[19] N. Goldman, J. C. Budich, and P. Zoller, Nat. Phys. **12**, 639 (2016).
[20] N. Fláschner, B. S. Rem, M. Tarnowski, D. Vogel, D.-S. Lúhmann, K. Sengstock, and C. Weitenberg, Science **352**, 1091 (2016).
[21] E. Alba, X. Fernandez-Gonzalvo, J. Mur-Petit, J. K. Pachos, and J. J. Garcia-Ripoll, Phys. Rev. Lett. **107**, 235301 (2011).
[22] P. Hauke, M. Lewenstein, and A. Eckardt, Phys. Rev. Lett. **113**, 045303 (2014).
[23] M. D. Caio, N. R. Cooper, and M. J. Bhaseen, Phys. Rev. Lett. **115**, 236403 (2015).
[24] L. D'Alessio and M. Rigol, Nat. Commun. **6**, 8336 (2015).
[25] C. Wang, P. Zhang, X. Chen, J. Yu, and H. Zhai, Phys. Rev. Lett. **118**, 185701 (2017).
[26] Y. Hu, P. Zoller, and J. C. Budich, Phys. Rev. Lett. **117**, 126803 (2016).
[27] J. H. Wilson, J. C. W. Song, and G. Refael, Phys. Rev. Lett. **117**, 235302 (2016).
[28] F. N. Ünal, E. J. Mueller, and M. Ö. Oktel, Phys. Rev. A **94**, 053604 (2016).
[29] P. Wang, M. Schmitt, and S. Kehrein, Phys. Rev. B **93**, 085134 (2016).
[30] J. Yu, Phys. Rev. A **96**, 023601 (2017).
[31] M. Tarnowski, F. Nur Ünal, N. Fläschner, B. S. Rem, A. Eckardt, K. Sengstock, and C. Weitenberg, arXiv:1709.01046.
[32] W. P. Su, J. R. Schrieffer, and A. J. Heeger, Phys. Rev. Lett. **42**, 1698 (1979).
[33] A. Y. Kitaev, Ann. Phys. (NY) **303**, 2 (2003).
[34] See Supplemental Material at http://link.aps.org/supplemental/10.1103/PhysRevB.97.060304 for calculations of the evolution of density matrices, the dynamical topological invariant, and the properties of fixed points.
[35] The crossing point belongs to two submanifolds at the same time [see the pink points ($k = k_1$ and k_2) in Fig. 1], so the total manifold is not the direct sum of each submanifold, but it does not impact the following definition of the dynamical topological invariant.
[36] A. P. Schnyder, S. Ryu, A. Furusaki, and A. W. W. Ludwig, Phys. Rev. B **78**, 195125 (2008); in *Advances in Theoretical Physics: Landau Memorial Conference*, edited by V. Lebedev and M. Feigel'man, AIP Conf. Proc. Vol. 1134 (AIP, Melville, NY, 2009), p. 10.
[37] A. Kitaev, in *Advances in Theoretical Physics: Landau Memorial Conference* (Ref. [36]), p. 22.
[38] L. Li, Z. Xu, and S. Chen, Phys. Rev. B **89**, 085111 (2014).
[39] C. Yang, H. Guo, L.-B. Fu, and S. Chen, Phys. Rev. B **91**, 125132 (2015).
[40] L. Li, C. Yang, and S. Chen, Eur. Phys. J. B **89**, 195 (2016).
[41] L. Li and S. Chen, Phys. Rev. B **92**, 085118 (2015).